

## Dynamic recovery and dynamic recrystallization of NiTi shape memory alloy under hot compression deformation

Shu-yong JIANG, Yan-qiu ZHANG, Ya-nan ZHAO

Industrial Training Centre, Harbin Engineering University, Harbin 150001, China

Received 14 November 2011; accepted 5 January 2012

**Abstract:** Mechanical behavior of nickel–titanium shape memory alloy (NiTi SMA) under hot deformation was investigated according to the true stress–strain curves of NiTi samples under compression at the strain rates of  $0.001\text{--}1\text{ s}^{-1}$  and at the temperatures of  $600\text{--}1000\text{ }^{\circ}\text{C}$ . Dynamic recovery and dynamic recrystallization of NiTi SMA were systematically investigated by microstructural evolution. The influence of the strain rates, the deformation temperatures and the deformation degree on the dynamic recovery and dynamic recrystallization of NiTi SMA was obtained as well. NiTi SMA was characterized by the combination of dynamic recovery and dynamic recrystallization at  $600\text{ }^{\circ}\text{C}$  and  $700\text{ }^{\circ}\text{C}$ , but the complete dynamic recrystallization occurred at other deformation temperatures. Increasing the deformation temperatures or decreasing the strain rates leads to larger equiaxed grains. The deformation degree has an important influence on the dynamic recrystallization of NiTi SMA. There exists the critical deformation degree during the dynamic recrystallization of NiTi SMA, beyond which the larger deformation degree contributes to obtaining the finer equiaxed grains.

**Key words:** NiTi alloy; shape memory alloy; dynamic recovery; dynamic recrystallization; hot deformation

### 1 Introduction

Nickel–titanium shape memory alloy (NiTi SMA) is widely used in engineering fields because of its shape memory effect as well as superelasticity [1,2]. Hot working plays an important role in the application of NiTi SMA to engineering fields. For example, many hot working methods, such as hot rolling, hot forging, hot extrusion, hot drawing, are the necessary approaches to transform as-cast NiTi ingots into NiTi bar, sheet, strip, tube and wire [3–5]. Hot working of NiTi SMA based on plastic deformation is of great importance in obtaining the perfect microstructure, which has a significant influence on the mechanical and functional properties of NiTi SMA [6–8]. Occurrence of dynamic recovery or dynamic recrystallization is unavoidable during the hot plastic deformation of NiTi SMA. Understanding the mechanism of dynamic recovery or dynamic recrystallization of NiTi SMA during the hot plastic deformation lays the foundations for obtaining the desired microstructure. MORAKABATI et al [9,10]

investigated hot tensile properties and microstructural evolution of as-cast NiTi SMA and found that at the temperatures ranging from  $800\text{ }^{\circ}\text{C}$  to  $1000\text{ }^{\circ}\text{C}$ , dynamic recrystallization is dominant, which is responsible for the high ductility of NiTi SMA [9,10]. KHAMEI and DEGHANI [11–13] established the constitutive behavior of  $\text{Ni}_{60}\text{Ti}_{40}$  (mass fraction, %) alloy at the temperatures ranging from  $950\text{ }^{\circ}\text{C}$  to  $1050\text{ }^{\circ}\text{C}$  and the strain rates ranging from  $0.001\text{ s}^{-1}$  to  $0.35\text{ s}^{-1}$  and investigated the influence of the Zener-Hollomon parameter on dynamic recrystallization of NiTi alloy. MORAKABATI et al [14,15] devoted themselves to obtaining the constitutive behavior of  $\text{Ni}_{49.8}\text{Ti}_{50.2}$  (mole fraction, %) alloy at the broader temperatures ranging from  $700\text{ }^{\circ}\text{C}$  to  $1000\text{ }^{\circ}\text{C}$  and at the broader strain rates ranging from  $0.001\text{ s}^{-1}$  to  $1\text{ s}^{-1}$  and investigated the influence of dynamic recovery and dynamic recrystallization on the hot workability of NiTi alloy [14,15].

In the present work, the dynamic recovery and dynamic recrystallization of NiTi SMA was systematically investigated according to the compression

tests at the strain rates ranging from  $0.001 \text{ s}^{-1}$  to  $1 \text{ s}^{-1}$  and at the temperatures ranging from  $600 \text{ }^\circ\text{C}$  to  $1000 \text{ }^\circ\text{C}$ .

## 2 Experimental

The as-received NiTi SMA with a nominal composition of  $\text{Ni}_{50.9}\text{Ti}_{49.1}$  (mole fraction, %) was prepared by vacuum induction melting method, and was then rolled at  $800 \text{ }^\circ\text{C}$ , and was drawn to the NiTi bar with a diameter of  $12 \text{ mm}$  at  $400 \text{ }^\circ\text{C}$ . The as-received NiTi bar was heated to  $850 \text{ }^\circ\text{C}$  for  $2 \text{ h}$ , followed by quenching into the ice water. The NiTi samples with a diameter of  $4 \text{ mm}$  and a height of  $6 \text{ mm}$  which were cut from the solution-treated NiTi bar by electro-discharge machining (EDM) were used for the compressive tests at various strain rates and temperatures. The microstructures of the as-received, the solution-treated and the compressed NiTi samples were observed by optical microscopy. All the specimens were etched in a solution containing HF,  $\text{HNO}_3$  and  $\text{H}_2\text{O}$ , whose volume ratio is  $V(\text{HF}):V(\text{HNO}_3):V(\text{H}_2\text{O})=1:4:5$ . Figure 1 demonstrates the optical microstructures of the as-received and solution-treated NiTi samples.

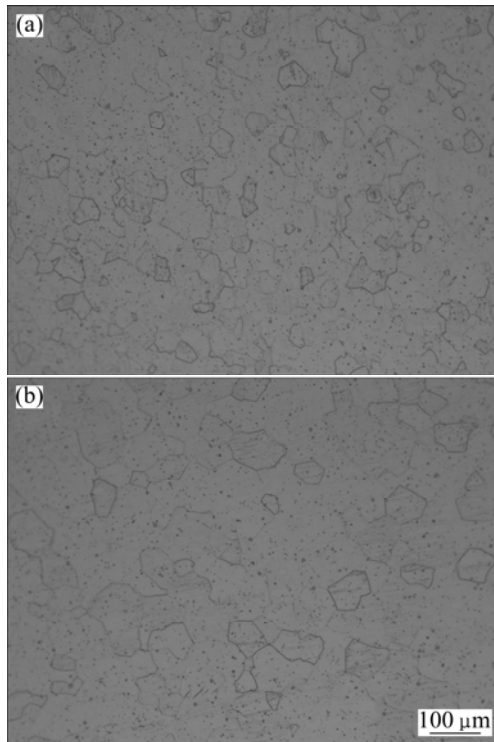


**Fig. 1** Optical microstructures of NiTi samples: (a) As-received; (b) Solution-treated

## 3 Results and discussion

### 3.1 Mechanical behavior of NiTi alloy under compression deformation

Figure 2 shows the true stress—strain curves of the

NiTi samples under the compression deformation of  $70\%$  at the strain rates of  $0.001\text{--}1 \text{ s}^{-1}$  and temperatures of  $600\text{--}1000 \text{ }^\circ\text{C}$ . It can be seen from Fig. 2 that the flow stresses of NiTi samples increase with increasing the strain rate and decrease with increasing the deformation temperature, which reveals that NiTi alloy is sensitive to the strain rate at elevated temperatures. Furthermore, all the stress—strain curves were characterized by dynamic recovery or dynamic recrystallization, which can be divided into three stages, namely working hardening, occurrence of dynamic recovery or dynamic recrystallization and final steady flow. Therefore, the dynamic recovery or dynamic recrystallization of NiTi alloy is unable to be judged only by the stress—strain curves and microstructure analysis is a necessary approach.

It is necessary to establish the constitutive equation to better describe the mechanical behavior of NiTi alloy under hot compression deformation. It is well known that the flow stress ( $\sigma$ ) can be expressed as a function of the strain ( $\varepsilon$ ), the strain rate ( $\dot{\varepsilon}$ ) and the temperature  $T$ , namely,

$$\sigma = \sigma(\varepsilon, \dot{\varepsilon}, T) \quad (1)$$

According to Eq. (1), the general form of the constitutive equation is described by

$$d\sigma = \left( \frac{\partial \sigma}{\partial \varepsilon} \right)_{\dot{\varepsilon}, T} d\varepsilon + \left( \frac{\partial \sigma}{\partial \dot{\varepsilon}} \right)_{\varepsilon, T} d\dot{\varepsilon} + \left( \frac{\partial \sigma}{\partial T} \right)_{\varepsilon, \dot{\varepsilon}} dT \quad (2)$$

where according to the compression or tension test, the first term  $(\partial \sigma / \partial \varepsilon)_{\dot{\varepsilon}, T}$  can be derived from a constant true strain-rate test, the second term  $(\partial \sigma / \partial \dot{\varepsilon})_{\varepsilon, T}$  can be derived from the strain-rate variation test, and the last term  $(\partial \sigma / \partial T)_{\varepsilon, \dot{\varepsilon}}$  can be derived from the temperature variation test.

In the case of large plastic strain, Eq.(2) can be expressed as

$$\frac{1}{\sigma} \frac{\partial \sigma}{\partial t} = \gamma \left( \frac{\partial \varepsilon}{\partial t} \right) + m \left( \frac{\partial \dot{\varepsilon}}{\partial t} / \frac{\partial \varepsilon}{\partial t} \right) + \frac{1}{\sigma} \frac{\partial \sigma}{\partial T} \frac{\partial T}{\partial t} \quad (3)$$

where  $\gamma = (1/\sigma)(\partial \sigma / \partial \varepsilon)$  is the strain softening rate, and  $m = (\dot{\varepsilon}/\sigma)(\partial \sigma / \partial \dot{\varepsilon})$  is the strain rate sensitivity.

However, the Arrhenius type equation is valid in describing the dependence of the flow stress of NiTi alloy on the temperature as well as the strain rate and is expressed as

$$\dot{\varepsilon} = A [\sinh(\alpha \sigma)]^n \exp \left( -\frac{Q}{RT} \right) \quad (4)$$

where  $Q$  is the activation energy,  $R$  is the universal gas constant, and  $A$ ,  $\alpha$  and  $n$  are the material constants.

In general, the Zener-Hollomon parameter  $Z$  represents the combined influence of the strain rate and

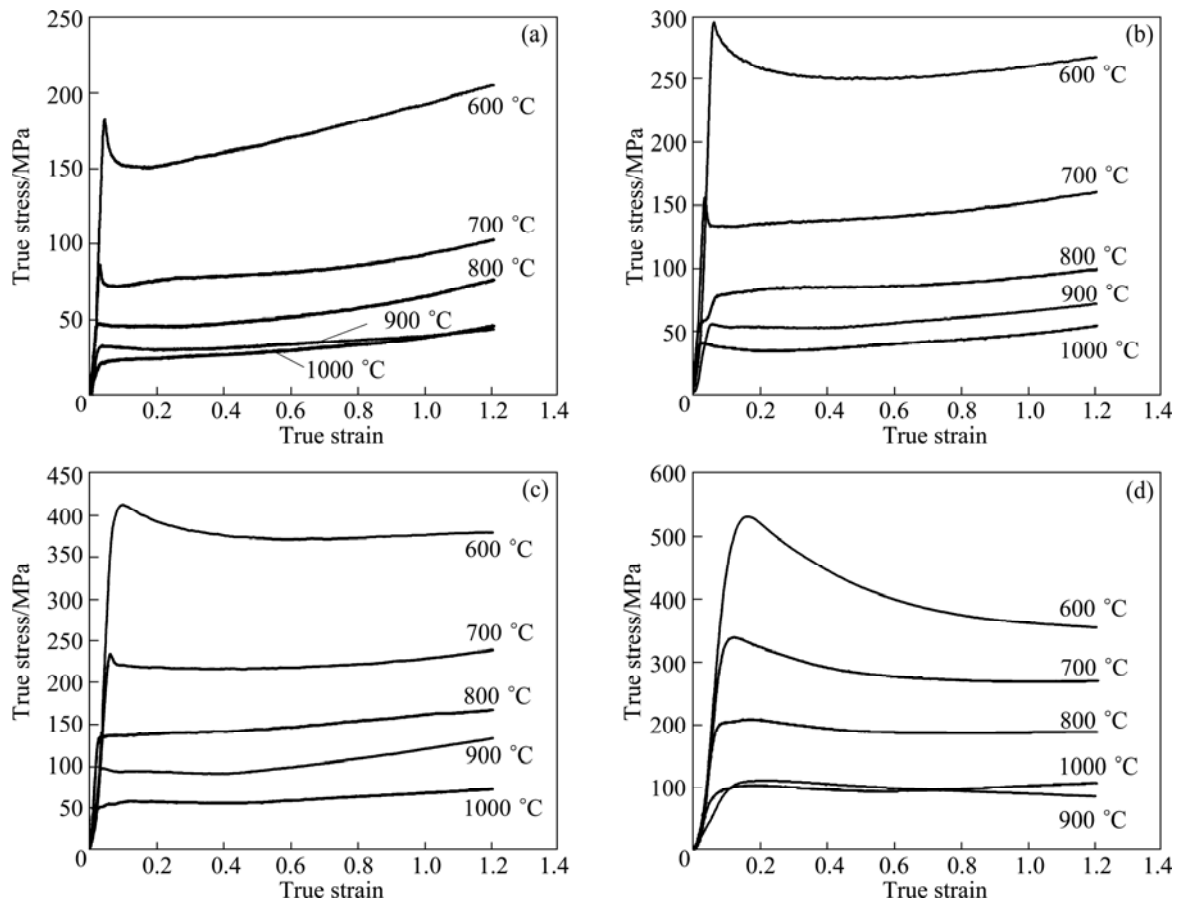


**Fig. 2** True stress—strain curves of NiTi alloy at different strain rates and temperatures: (a)  $0.001 \text{ s}^{-1}$ ; (b)  $0.01 \text{ s}^{-1}$ ; (c)  $0.1 \text{ s}^{-1}$ ; (d)  $1 \text{ s}^{-1}$

the temperature on the flow stress of NiTi alloy during the hot deformation and is expressed as

$$Z = \dot{\epsilon} \exp\left(\frac{Q}{RT}\right) \quad (5)$$

Substitution Eq. (5) into Eq. (4) results in

$$Z = A[\sinh(\alpha\sigma)]^n \quad (6)$$

Based on the stress—strain curves in Fig. 2, the constitutive equation of NiTi alloy can be obtained, which will be published in another literature.

### 3.2 Microstructural evolution of NiTi alloy at different temperatures and strain rates

The microstructural evolution of NiTi samples under compression deformation at the strain rates ranging from  $0.001 \text{ s}^{-1}$  to  $1 \text{ s}^{-1}$  and at the temperatures ranging from  $600 \text{ }^\circ\text{C}$  to  $1000 \text{ }^\circ\text{C}$  is observed in order to further understand the dynamic recovery or dynamic recrystallization, as shown in Figs. 3–7. It can be seen from Fig. 3 to Fig. 7 that the microstructure of the NiTi samples at  $600 \text{ }^\circ\text{C}$  is considerably different from that at the other temperatures. The former seems to be characterized by the combination of dynamic recovery

and dynamic recrystallization, but the dynamic recovery is dominant since the grains are obviously elongated. The microstructure of the NiTi samples at  $700 \text{ }^\circ\text{C}$  reveals that almost complete dynamic recrystallization occurs at the strain rates of  $0.001 \text{ s}^{-1}$  and  $0.01 \text{ s}^{-1}$ , but the dynamic recovery prevails at the strain rates of  $0.1 \text{ s}^{-1}$  and  $1 \text{ s}^{-1}$ . However, the microstructures of the NiTi samples at the other temperatures exhibit complete dynamic recrystallization. While both the dynamic recovery and dynamic recrystallization are characterized by the simultaneous occurrence of working hardening and dynamic softening, the softening mechanism of the two is considerably distinct. The softening mechanism of the dynamic recovery is based on the climb of edge dislocations, cross-slip of screw dislocations and counteraction of unlike dislocations, which contributes to lowering the dislocation density. However, the softening mechanism of dynamic recrystallization is attributed to the nucleation and growth of new grains resulting from the dynamic recrystallization. The balance between working hardening and dynamic softening results in the steady flow of NiTi alloy during the hot deformation.

The strain rates and the deformation temperatures have an important influence on the dynamic recovery

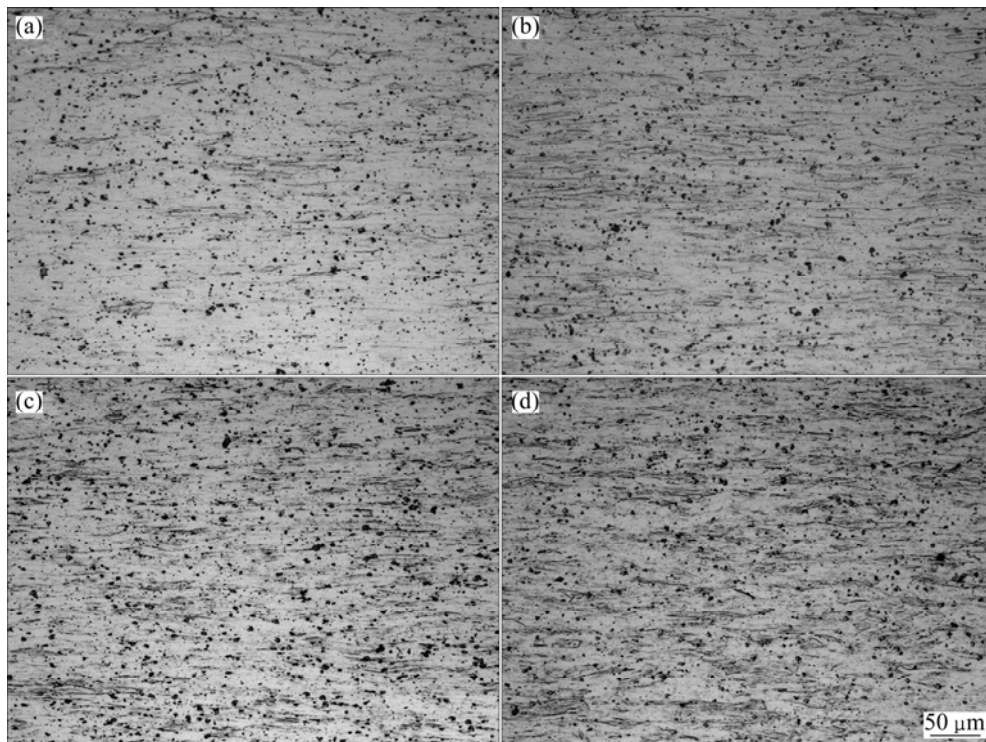


**Fig. 3** Optical microstructures of NiTi samples under compression at 600 °C: (a) 0.001 s<sup>-1</sup>; (b) 0.01 s<sup>-1</sup>; (c) 0.1 s<sup>-1</sup>; (d) 1 s<sup>-1</sup>

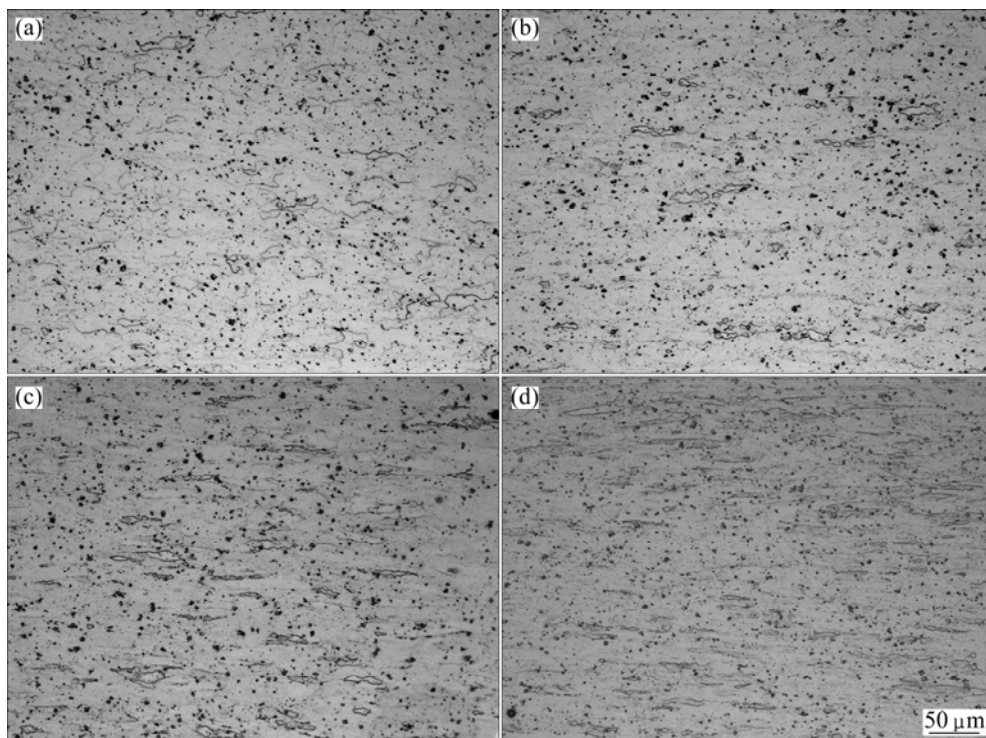


**Fig. 4** Optical microstructures of NiTi samples under compression at 700 °C: (a) 0.001 s<sup>-1</sup>; (b) 0.01 s<sup>-1</sup>; (c) 0.1 s<sup>-1</sup>; (d) 1 s<sup>-1</sup>

and dynamic recrystallization of NiTi alloy. In general, the lower strain rates and the higher temperatures provide longer time for energy accumulation and higher interface migration for the nucleation and growth of dynamically recrystallized grains as well as dislocation annihilation, which contributes to lowering the flow

stress of the NiTi alloy.

In addition, the strain rates and the deformation temperatures have remarkable effects on the size of the grains from dynamic recrystallization. It can be seen from Fig. 5 to Fig. 7 that increasing the deformation temperature or decreasing the strain rate contributes to

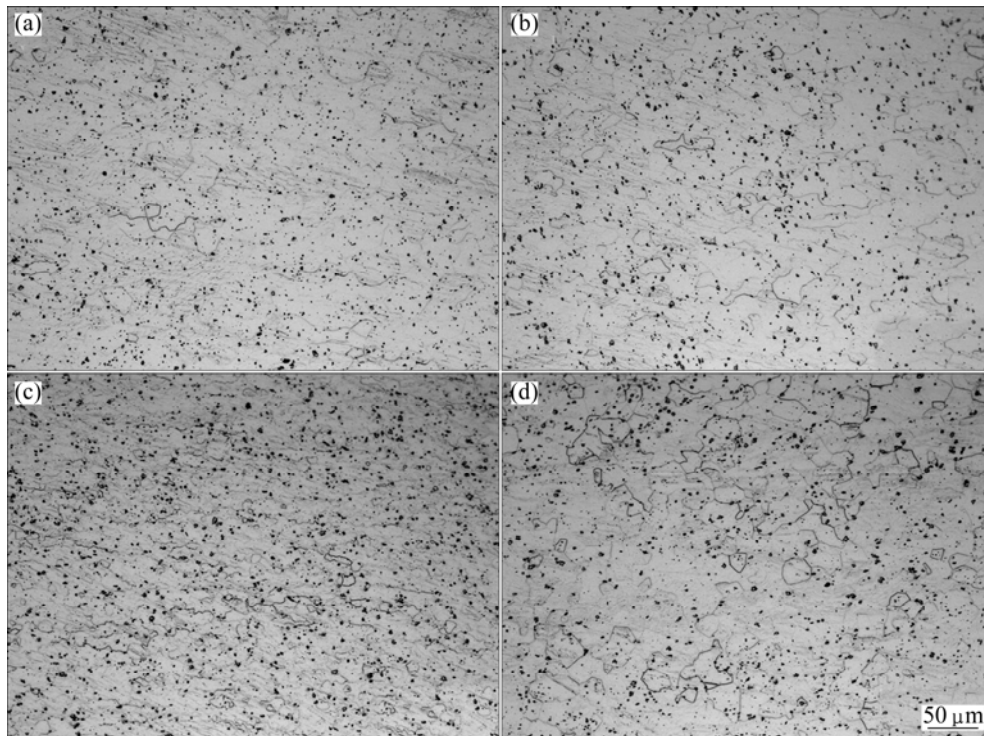


**Fig. 5** Optical microstructures of NiTi samples under compression at 800 °C: (a)  $0.001 \text{ s}^{-1}$ ; (b)  $0.01 \text{ s}^{-1}$ ; (c)  $0.1 \text{ s}^{-1}$ ; (d)  $1 \text{ s}^{-1}$

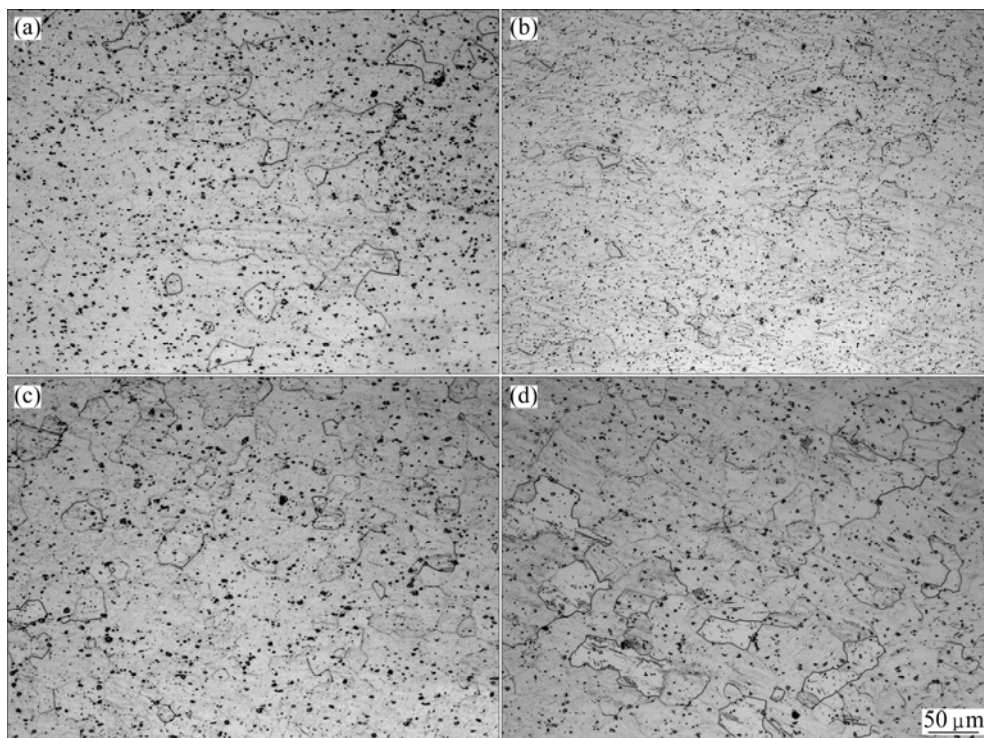


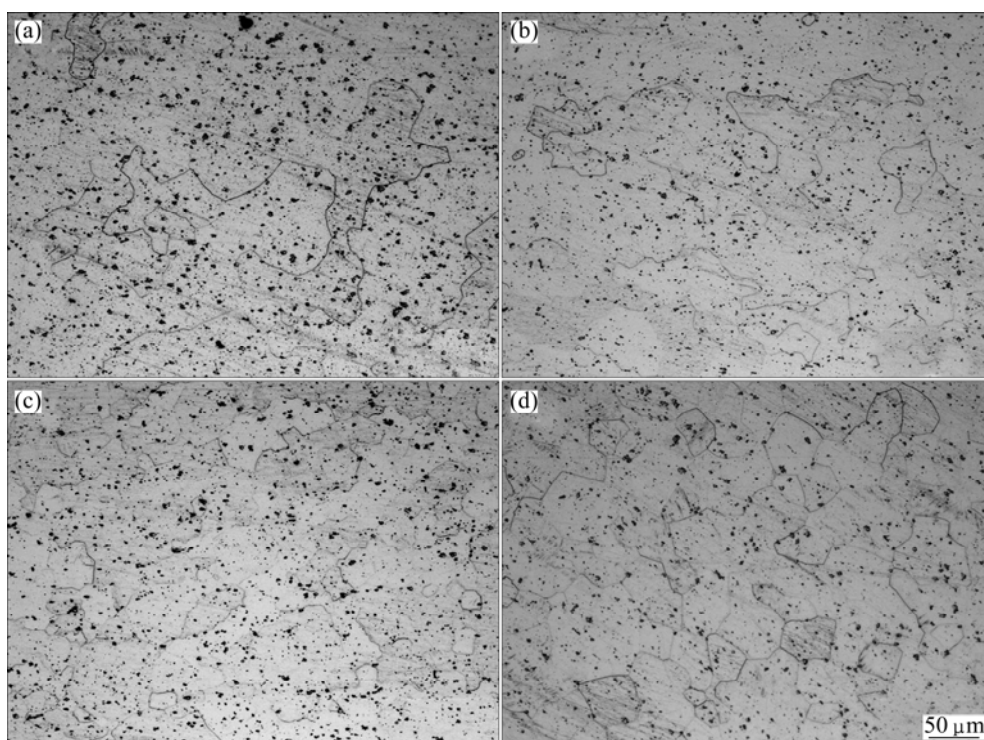
**Fig. 6** Optical microstructures of NiTi samples under compression at 900 °C: (a)  $0.001 \text{ s}^{-1}$ ; (b)  $0.01 \text{ s}^{-1}$ ; (c)  $0.1 \text{ s}^{-1}$ ; (d)  $1 \text{ s}^{-1}$

obtaining the large equiaxed grains.

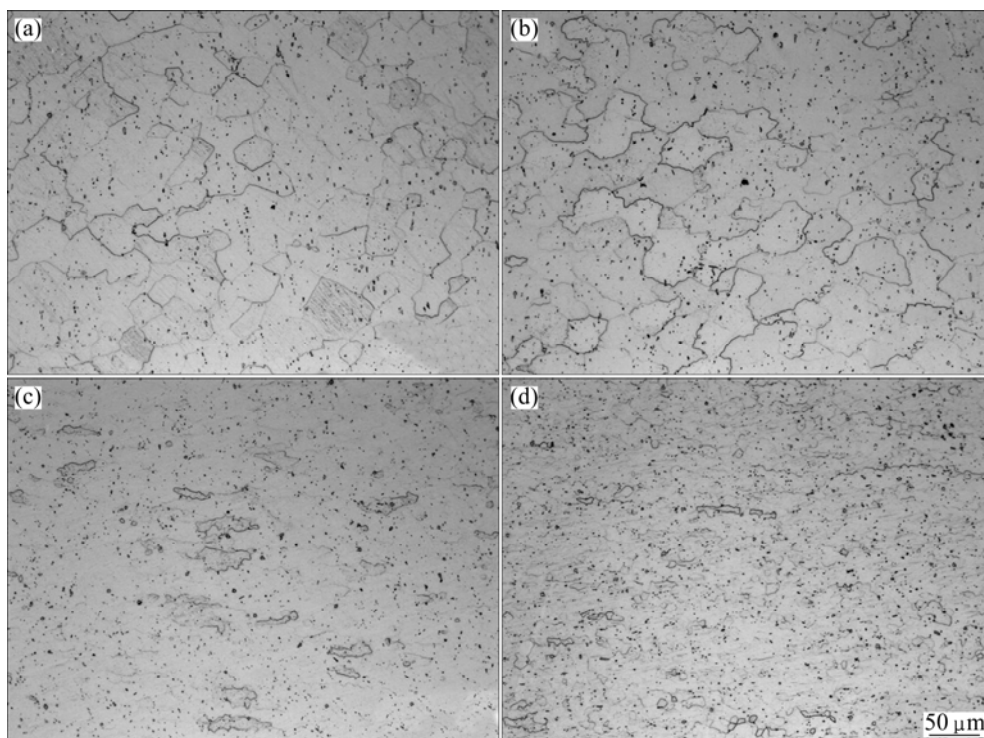
### 3.3 Microstructural evolution of NiTi alloy at different deformation degrees

Figure 8 shows the microstructures of the NiTi samples at the compression deformation degrees of 10%,

30%, 50% and 90%, respectively. It can be seen from Fig. 8 and Fig. 5(c) that microstructures of NiTi alloy at the compression deformation degrees of 10% and 30% are characterized by the much coarser recrystallized grains, but the size of the recrystallized grains decreases with the increase of the strain at the compression deformation



**Fig. 7** Optical microstructures of NiTi samples under compression at 1000 °C: (a)  $0.001 \text{ s}^{-1}$ ; (b)  $0.01 \text{ s}^{-1}$ ; (c)  $0.1 \text{ s}^{-1}$ ; (d)  $1 \text{ s}^{-1}$



**Fig. 8** Optical microstructures of NiTi samples under compression at temperature of 800 °C and strain rate of  $0.1 \text{ s}^{-1}$  at different deformation degrees: (a) 10%; (b) 30%; (c) 50%; (d) 90%

degrees of 50%, 70% and 90%, respectively. Accordingly, it can be concluded that the deformation degree has an important influence on the dynamic recrystallization of the NiTi alloy. In general, there exist two critical deformation degrees of  $\varepsilon_1$  and  $\varepsilon_2$ . When the deformation

degree is less than  $\varepsilon_1$ , there is no occurrence of dynamic recrystallization. When the deformation degree is between  $\varepsilon_1$  and  $\varepsilon_2$ , dynamic recrystallization takes place, but the recrystallized grains are very coarse. When the deformation degree is greater than  $\varepsilon_2$ , the recrystallized

grains are gradually refined with the increase of the strain. It can be seen from the stress—strain curves in Fig. 2 that the values of the two critical deformation degrees are associated with the deformation temperatures and the strain rates. In general, the two critical deformation degrees decrease with the increase of the deformation temperature and increase with the increase of the strain rate. The compression deformation degrees of 10% and 30% will belong to the range from  $\varepsilon_1$  to  $\varepsilon_2$ , but the compression deformation degrees of 50%, 70% and 90% are greater than  $\varepsilon_2$ , respectively.

When the deformation degree is less than  $\varepsilon_1$ , the accumulation of energy is unable to provide a sufficient driving force for the nucleation of dynamically recrystallized grains in the NiTi sample. When the deformation degree is between  $\varepsilon_1$  and  $\varepsilon_2$ , along with the increase of the intracrystalline and intercrystalline deformation, the nucleation of dynamically recrystallized grains occurs, but there is a small amount of nucleation centers. The local damage in the intercrystalline substance leads to the contact of the adjacent grains, which contributes to the bonding of the atoms in the original grains with the counterparts in the dynamically recrystallized grains, and finally a few grains merge into large grains. When the deformation degree is greater than  $\varepsilon_2$ , a great number of nucleation centers arise along with the increase of the deformation and thus the number of the dynamically recrystallized grains increases considerably, so the dynamically recrystallized grains are very fine.

## 4 Conclusions

1) The flow stress of NiTi alloy depends on the strain rate and the deformation temperature and increases with increasing the strain rate and decreases with increasing the deformation temperature.

2) The microstructure of NiTi alloy at 600 °C is characterized by the combination of dynamic recovery and dynamic recrystallization, but the dynamic recovery is dominant since the grains are obviously elongated. The microstructure of NiTi samples at 700 °C reveals that almost complete dynamic recrystallization occurs at the strain rates of  $0.001 \text{ s}^{-1}$  and  $0.01 \text{ s}^{-1}$ , but the dynamic recovery prevails at the strain rates of  $0.1 \text{ s}^{-1}$  and  $1 \text{ s}^{-1}$ . The microstructures of NiTi samples at 800–1000 °C exhibit complete dynamic recrystallization. Increasing the deformation temperature or decreasing the strain rate contributes to obtaining larger equiaxed grains.

3) In general, there exist two critical deformation degrees of  $\varepsilon_1$  and  $\varepsilon_2$ . When the deformation degree is less than  $\varepsilon_1$ , there is no occurrence of dynamic recrystallization. When the deformation degree is between  $\varepsilon_1$  and  $\varepsilon_2$ , dynamic recrystallization takes place

and the recrystallized grains are very coarse. The compression deformation degrees of 10% and 30% will belong to the range from  $\varepsilon_1$  to  $\varepsilon_2$ , but the compression deformation degrees of 50%, 70% and 90% are greater than  $\varepsilon_2$ , respectively. Therefore, the dynamically recrystallized grains are very coarse at the compression deformation degrees of 10% and 30%, but the size of the dynamically recrystallized grains decreases with the increase of the strain at the compression deformation degrees of 50%, 70% and 90%, respectively.

## References

- [1] OTUKA K, REN X. Physical metallurgy of Ti–Ni-based shape memory alloys [J]. *Progress in Materials Science*, 2005, 50(5): 511–678.
- [2] SUN L, HUANG W M, DING Z, ZHAO Y, WANG C C, PURNAWALI H, TANG C. Stimulus-responsive shape memory materials: A review [J]. *Materials and Design*, 2012, 33(1): 577–640.
- [3] MEHRABI K, BAHMANPOUR H, SHOKUH FAR A, KNEISSL A. Influence of chemical composition and manufacturing conditions on properties of NiTi shape memory alloys [J]. *Materials Science and Engineering A*, 2008, 481–482: 693–696.
- [4] KUTITA T, MATSUMOTO H, ABE H. Transformation behavior in rolled NiTi [J]. *Journal of Alloys and Compounds*, 2004, 381: 158–161.
- [5] FRICK C P, ORTEGA A M, TYBER J, MAKSOUD A E M, MAIER H J, LIU Y N, GALL K. Thermal processing of polycrystalline NiTi shape memory alloys [J]. *Materials Science and Engineering A*, 2005, 405(1–2): 34–49.
- [6] LI Zhen-hua, XIANG Cuo-quan, CHENG Xian-hua. Effects of ECAE process on microstructure and transformation behavior of TiNi shape memory alloy [J]. *Materials and Design*, 2006, 27(4): 324–328.
- [7] GALL K, TYBER J, WILKESANDERS G, ROBERTSON S W, RITCHIE R O, MAIER H J. Effect of microstructure on the fatigue of hot-rolled and cold-drawn NiTi shape memory alloys [J]. *Materials Science and Engineering A*, 2008, 486(1–2): 389–403.
- [8] SADRNEZHAAD S K, MIRABOLGHASEMI S H. Optimum temperature for recovery and recrystallization of 52Ni48Ti shape memory alloy [J]. *Materials and Design*, 2007, 28(6): 1945–1948.
- [9] MORAKABATI M, ABOUTALEBI M, KHEIRANDISH S, KARIMI TAHERI A, ABBASI S M. Hot tensile properties and microstructural evolution of as cast NiTi and NiTiCu shape memory alloys [J]. *Materials and Design*, 2011, 32(4): 406–413.
- [10] MORAKABATI M, KHEIRANDISH S, ABOUTALEBI M, KARIMI TAHERI A, ABBASI S M. The effect of Cu addition on the hot deformation behavior of NiTi shape memory alloys [J]. *Journal of Alloys and Compounds*, 2010, 499(1): 57–62.
- [11] KHAMEI A A, DEGHANI K. Modeling the hot-deformation behavior of Ni<sub>60wt%</sub>-Ti<sub>40wt%</sub> intermetallic alloy [J]. *Journal of Alloys and Compounds*, 2010, 490(1–2): 377–381.
- [12] KHAMEI A A, DEGHANI K. A study on the mechanical behavior and microstructural evolution of Ni<sub>60wt%</sub>-Ti<sub>40wt%</sub> (60Nitinol) intermetallic compound during hot deformation [J]. *Materials Chemistry and Physics*, 2010, 123(1): 269–277.
- [13] DEGHANI K, KHAMEI A A. Hot deformation behavior of 60Nitinol (Ni<sub>60wt%</sub>-Ti<sub>40wt%</sub>) alloy: Experimental and computational studies [J]. *Materials Science and Engineering A*, 2010, 527(3): 684–690.
- [14] MORAKABATI M, KHEIRANDISH S, ABOUTALEBI M, KARIMI TAHERI A, ABBASI S M. A study on the hot workability

of wrought NiTi shape memory alloy [J]. Materials and Science Engineering A, 2011, 528(18): 5656–5663.

KARIMI TAHERI A, ABBASI S M. High temperature deformation and processing map of a NiTi intermetallic alloy [J]. Intermetallics, 2011, 19(10): 1399–1404.

[15] MORAKABATI M, ABOUTALEBI M, KHEIRANDISH S,

## 镍钛形状记忆合金在热压缩变形下的 动态回复和动态再结晶

江树勇, 张艳秋, 赵亚楠

哈尔滨工程大学 工程训练中心, 哈尔滨 150001

**摘 要:** 通过获得镍钛形状记忆合金在应变速率( $0.001\sim 1\text{ s}^{-1}$ )和变形温度( $600\sim 1000\text{ }^{\circ}\text{C}$ )下的压缩真实应力—应变曲线, 研究镍钛形状记忆合金在热变形下的力学行为。通过显微组织演变研究镍钛形状记忆合金的动态回复和动态再结晶, 获得应变速率、变形温度和变形程度对镍钛形状记忆合金的动态回复和动态再结晶的影响规律。镍钛形状记忆合金在  $600\text{ }^{\circ}\text{C}$  和  $700\text{ }^{\circ}\text{C}$  下, 动态回复和动态再结晶共存, 但在其他温度下表现出完全动态再结晶。增加变形温度或降低应变速率, 导致较大的等轴晶粒。变形程度对镍钛形状记忆合金的动态再结晶具有重要的影响。在镍钛形状记忆合金的动态再结晶中存在临界变形程度, 当大于临界变形程度时, 较大的变形程度有助于获得细小的等轴再结晶晶粒。

**关键词:** 镍钛合金; 形状记忆合金; 动态回复; 动态再结晶; 热变形

(Edited by Xiang-qun LI)